Chinese Chemical Society · ICCAS · ROYAL SOCIETY OF CHEMISTRY

RESEARCH ARTICLE

Check for updates

Rational design of ratiometric and lysosome-targetable AIE dots for imaging endogenous HClO in live cells†

Yongxiang Hong,[ab] Hong Wang,[b] Mingju Xue,[b] Peisheng Zhang, (iD) *[bc] Wanqiang Liu,[b] Shu Chen,[b] Rongjin Zeng,[b] Jiaxi Cui,[de] Yong Gao (iD) *[a] and Jian Chen (iD) *[b]

Rational design of novel ratiometric and targetable fluorescent probes for selective imaging of lysosomal hypochlorous acid (HClO) is conducive to investigating the function of HClO in pathophysiological processes. Herein, we for the first time combine 1-pyrenecarboxaldehyde (with a $\pi-\pi$ stacking effect) and 2-methylquinoline derivatives to synthesize an aggregation-induced-emission (AIE) probe (**SA-C2-PCD**) for ratiometric detection of HClO in living cells. Subsequently, a kind of novel lysosome-targetable AIE dot (**AIED-Lyso**) with dual emission features is prepared via a simple co-precipitation of a lysosome-targeting surfactant MAA-CO720, an amphiphilic block copolymer PEO_{113}-b-PS_{46} and the HClO-responsive probe (**SA-C2-PCD**). The free **AIED-Lyso** shows only strong red AIE fluorescence without addition of HClO. However, when exposed to HClO, a strong oxidizing agent, the **SA-C2-PCD** would release 1-pyrenecarboxaldehyde that aggregates through $\pi-\pi$ stacking interaction in aqueous solutions, inducing a distinct fluorescence change from red to blue. Interestingly, the as-prepared **AIED-Lyso** displays good water dispersity, high selectivity and sensitivity ($\sim$70.4 nM), strong anti-interference ability, prominent long-term fluorescence stability ($>$10 weeks), and low cytotoxicity, and it can be successfully applied to visually detect endogenous lysosomal HClO in live cells.

Introduction

Hypochlorous acid (HClO) is known as an active oxygen molecule that is mainly produced by hydrogen peroxide and chloride ions under the catalysis of myeloperoxidase (MPO) and it also plays an important role in fighting pathogenic microorganisms, resisting viruses, *etc.*[1,2] Abnormal levels of endogenous HClO can cause a series of diseases, including Parkinson's disease, Alzheimer's disease, cancer, *etc.*[3,4] On the other hand, lysosomes, as an acidic organelle (pH 4.5–5.5), have long been considered as a waste disposal facility in cells.[5] Recent studies have shown that lysosomes possess various biological functions, including cell signal transduction, protein degradation, plasma membrane repair, homogenous stability, and autophagy, and are regarded as critical subcellular organelles.[6,7] Lysosomes are one of the main HClO-producing organelles, and excess HClO can induce cell death through calpain activation and lysosomal disruption.[8,9] Therefore, qualitative analysis and detection of HClO in lysosomes are of great significance.

The recently developed fluorescence method has the merits of simple operation, rapid real-time analysis, and high spatial and temporal resolution, and has received extensive attention and significant development.[10–18] To date, a series of small molecule-based fluorescent probes for optically sensing HClO have been fabricated.[19–22] However, most of them show a single fluorescence signal that often varies with other factors such as microenvironment, sensor concentration, photobleaching, and excitation intensity and thus the reliability could be low.[23–25]

[a] College of Chemistry and Key Laboratory of Polymeric Materials & Application Technology of Hunan Province, and Key Laboratory of Advanced Functional Polymeric Materials of College of Hunan Province, Xiangtan University, China. E-mail: gydx.1027@163.com

[b] Key Laboratory of Theoretical Organic Chemistry and Functional Molecule of Ministry of Education, Hunan Provincial Key Laboratory of Controllable Preparation and Functional Application of Fine Polymers, Hunan Province College Key Laboratory of QSAR/QSPR, Hunan Provincial Key Lab of Advanced Materials for New Energy Storage and Conversion, School of Chemistry and Chemical Engineering, Hunan University of Science and Technology, Xiangtan, Hunan 411201, China. E-mail: cj0066@gmail.com, pshzhang07@gmail.com

[c] State Key Laboratory of Chemo/Biosensing and Chemometrics, Hunan University, Changsha 410082, P. R. China

[d] INM-Leibniz Institute for New Materials Campus D2 2, 66123 Saarbrícken, Germany

[e] Institute of Fundamental and Frontier Sciences, University of Electronic Science and Technology of China, Chengdu, Sichuan, 610054, China

† Electronic supplementary information (ESI) available: Synthesis procedures, ^{1}H NMR spectra, ^{13}C NMR, MS, absorption spectrum, fluorescence spectra, AIE behaviour, detection limit, cell viability, *etc.* See DOI: 10.1039/c8qm00511g

This journal is © The Royal Society of Chemistry and the Chinese Chemical Society 2019

Mater. Chem. Front., 2019, **3**, 203–208 | 203

In contrast, signals containing two well-resolved emissions (ratiometric) from fluorescent probes can effectively increase the accuracy.[26–31] However, most of the strategies currently available are built on the use of conventional small molecule-based ratiometric probes which usually show the undesirable aggregation-induced quenching (ACQ) phenomenon in aqueous solutions, significantly confining their detection performance.[32–34] In addition, the self-absorption effect of these reported conventional small fluorescent probes due to their small Stokes shift also leads to fluorescence self-annihilation.[35]

Currently, aggregation-induced-emission (AIE) based fluorophores, which were first developed by Tang and co-workers, are proving to be effective probes avoiding the ACQ effect.[36–42] In particular, the AIE dots developed very recently are widely used as novel fluorescent probes in the field of sensing and imaging in living cancer cells due to their outstanding merits such as stable dispersity in water, large Stokes shift, intense fluorescence, prominent photostability, good biocompatibility, etc.[43–47] However, to the best of our knowledge, no lysosome-targetable AIE dots for ratiometric detection of lysosomal HClO have been reported yet.

In this study, we report on the construction of lysosome-targetable AIE dots (**AIED-Lyso**) for ratiometric imaging of lysosomal HClO. Our AIE dots are made via a simple co-precipitation of a lysosome-targetable surfactant MAA-CO720, an amphiphilic block copolymer PEO_{113}-b-PS_{46} and a HClO-responsive probe (**SA-C2-PCD**), as shown in Scheme 1. In our design, in the presence of strong oxidant HClO, the double bond of **SA-C2-PCD** would break to reduce its red AIE fluorescence and also generate 1-pyrenecarboxaldehyde. This new-born chromophore would induce a progressively enhanced blue fluorescence due to intermolecular π–π stacking interaction. The as-prepared **AIED-Lyso** with good biocompatibility can mainly locate in lysosomes, and monitor endogenous HClO in lysosomes.

Experimental section
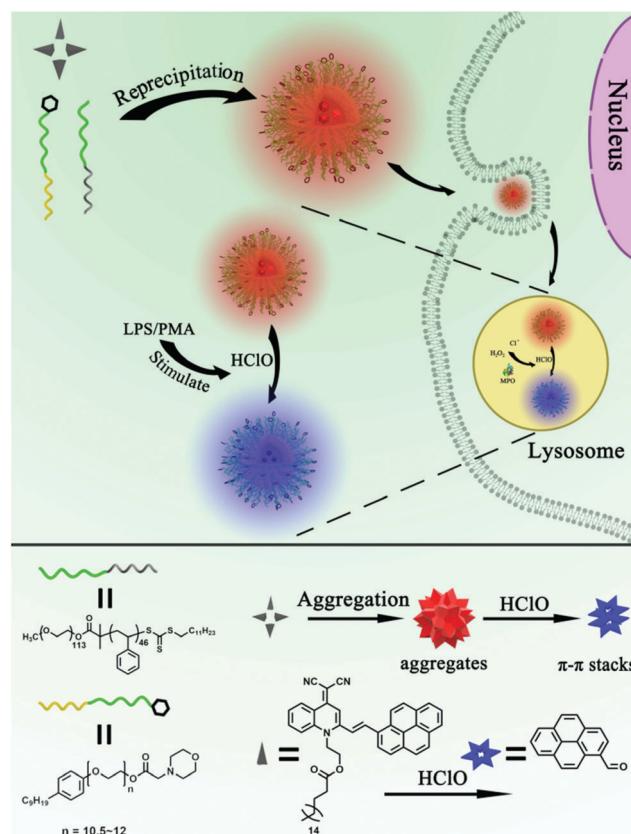
Materials and instruments

All the chemical agents were purchased from commercial sources. Compound **1**, compound **2** and PEO_{113}-b-PS_{46} were synthesized via the protocols developed by us.[48] The synthesis, apparatus, cytotoxicity and live cell imaging were as stated in the ESI.†

Results and discussion

The strategy for the fabrication of AIED-Lyso

Scheme 1 depicts the strategy for fabricating **AIED-Lyso**. We take advantage of the prominent AIE nature of **SA-C2-PCD** to alternate the undesirable ACQ effect and also get a large Stokes shift (∼220 nm) for avoiding self-absorption interference. An amphiphilic block copolymer (PEO_{113}-b-PS_{46}) is designed to provide a hydrophobic environment by forming micelles to enhance the long-term stability, photostability, and brightness of the hydrophobic AIE dyes. When additional morpholine groups are incorporated, these micelle-based particles could serve as the targetable vehicles for specific targeting of lysosomes.

Scheme 1 Ratiometric imaging of endogenous HClO in lysosomes using lysosome-targetable AIE dots (**AIED-Lyso**).

The synthesis of **SA-C2-PCD** and MAA-CO720 is described in Schemes S1 and S2 (ESI†). All the intermediates and the final product were characterized by ^{1}H NMR, ^{13}C NMR and mass spectroscopy (Fig. S1–S5, ESI†).

Well-dispersed **AIED-Lyso** was synthesized via a co-precipitation strategy (Scheme 1) in which all these components were dissolved in THF at first and then co-precipitated in water to form nanoparticles. The core of the nanoparticles is composed of hydrophobic compositions including **SA-C2-PCD**, PS, and nonylphenyl groups, while the shell is made from hydrophilic PEO groups. In this structure, the morphoyl terminal groups can not only improve water solubility, but also specifically locate at lysosomes. The obtained **AIED-Lyso** are spherical with an average diameter of 30 nm (checked by transmission electron microscope (TEM) and dynamic light scattering (DLS), Fig. 1A and B). For the fluorescence long-term stability test, the diluted **AIED-Lyso** dispersion was sealed and stored in the dark under an ambient temperature. Then an aliquot was drawn out for the fluorescence test every week. As shown in Fig. S6 (ESI†), the fluorescence intensity ratio (F_{475}/F_{620}) of the diluted **AIED-Lyso** sample without and with HClO changed seldom even after storing for 10 weeks, implying its remarkable long-term stability of fluorescence. In addition, the average diameter of the **AIED-Lyso** dispersion at different time slots was provided (Fig. S7, ESI†). No obvious size changes in the **AIED-Lyso** dispersion were observed even after storing for 10 weeks, indicating the admirable stability of our nanoprobe.
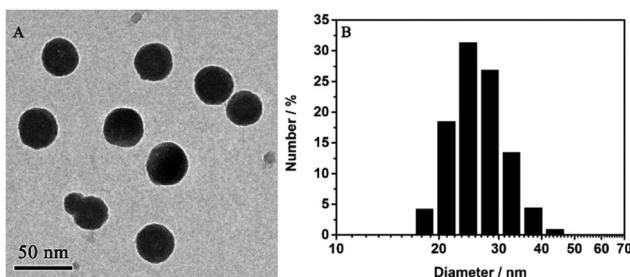
Fig. 1 (A) TEM image of **AIED-Lyso**; (B) size of **AIED-Lyso** determined by DLS.

Ratiometric detection of HClO

We first tested the fluorescence of **SA-C2-PCD** under different conditions (THF/water mixture) to confirm its AIE property (Fig. S8, ESI†). In THF, a good solvent for **SA-C2-PCD**, no visible fluorescence was observed. When water was added to induce aggregation, the relative emission intensity (F_0/F) of **SA-C2-PCD** gradually increased at first (water fractions $f_w < 80$ vol%) and then jumped at $f_w > 80$ vol%, showing a F_0/F of 198 at $f_w = 95$ vol%, indicating a typical AIE effect.

We then investigated the responsiveness of **AIED-Lyso** to HClO. Note that **AIED-Lyso** itself exhibited an obvious absorption peak at 440 nm in the solution state. When HClO was added, the peak at 440 nm gradually declined, accompanied by the formation of an increasing new absorption peak centered at 350 nm (Fig. S9, ESI†). Simultaneously, as shown in Fig. 2A and B (Fig. S10, ESI†), obvious blue-shift from 620 nm to 475 nm was observed in the emission spectra, suggesting a reliable ratiometric detection mode. Moreover, the fluorescence intensity ratio (F_{475}/F_{620}) varies linearly with HClO concentration (0–5 μM) with a detection limit of 70.4 nM (Fig. S11, ESI†).
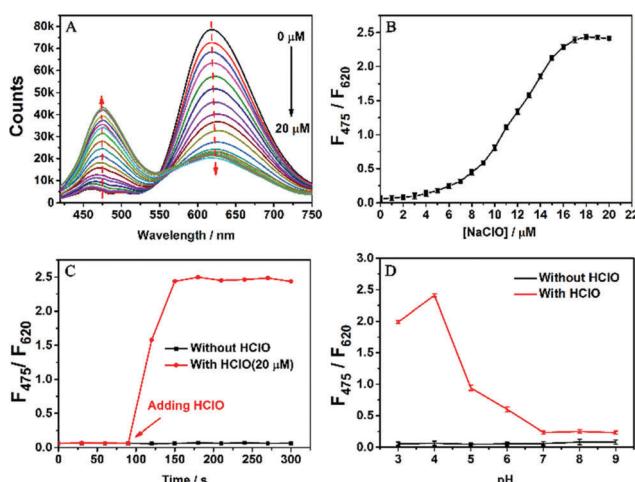
Fig. 2 (A) Fluorescence response of **AIED-Lyso** (2.67 μg mL^{-1}) towards different concentrations of HClO (0–20 μM, λ_{ex} = 399 nm); (B) the fluorescence intensity ratio (F_{475}/F_{620}) as a function of HClO concentration (0–20 μM); (C) the fluorescence intensity ratio (F_{475}/F_{620}) as a function of time; and (D) the fluorescence intensity ratio (F_{475}/F_{620}) without and with HClO (20 μM) as a function of pH.
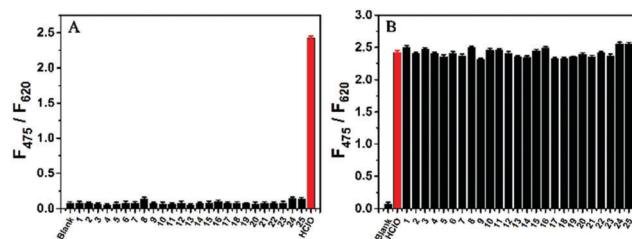
Fig. 3 (A) Fluorescence intensity ratio (F_{475}/F_{620}) for **AIED-Lyso** (2.67 μg mL^{-1}) in the presence of 20 μM HClO or one biologically relevant molecule; (B) fluorescence intensity ratio (F_{475}/F_{620}) for **AIED-Lyso** (2.67 μg mL^{-1}) in the presence of 20 μM of HClO and one biologically relevant molecule; note: (1–18 : 200 μM, 19–20 : 5.0 mM, 21–25 : 200 μM) 1, Na$^+$; 2, K$^+$; 3, Ca^{2+}; 4, Zn^{2+}; 5, Co^{2+}; 6, Cu^{2+}; 7, Mg^{2+}; 8, Fe^{3+}; 9, Fe^{2+}; 10, Ni^{2+}; 11, Cl$^-$; 12, SO$_4^{2-}$; 13, NO$_3^-$; 14, H$_2$PO$_4^-$; 15, HPO$_4^{2-}$; 16, PO$_4^{3-}$; 17, SO$_3^{2-}$; 18, NO$_2^-$; 19, Cys; 20, GSH; 21, H$_2$O$_2$; 22, NO; 23, ^{1}O$_2$; 24, HO; 25, t-BuO. λ_{ex} = 399 nm.

Fig. 2C shows the time response of the nanoprobe toward HClO. The F_{475}/F_{620} ratio changed after HClO was added into the **AIED-Lyso** solution for only one min, implying a rapid detection feature. Fig. 2D describes the effect of pH on the fluorescence intensity ratio (F_{475}/F_{620}) in the absence and presence of HClO. Without HClO, **AIED-Lyso** exhibits good stability from pH 3.0 to 9.0. In contrast, the addition of HClO (20 μM) induces an obvious enhancement of F_{475}/F_{620} from pH 3.0 to 6.0, suggesting the wide adaptive range of **AIED-Lyso** in acidic environments including lysosomes.

To evaluate the selectivity of **AIED-Lyso**, the F_{475}/F_{620} ratio of **AIED-Lyso** solution was examined in the presence of HClO or other biologically relevant molecules including anions, reactive oxygen species (ROS) and thiols (Fig. 3A). Except for HClO, other biologically relevant molecules did not induce obvious variation in F_{475}/F_{620}. Moreover, a negligible interfering effect on the F_{475}/F_{620} ratio of **AIED-Lyso** was found when HClO and other biologically relevant molecules were added together (Fig. 3B). All these results indicated that **AIED-Lyso** can selectively detect HClO in complex biological environments.

On the basis of the fluorescent response of **SA-C2-PCD** toward HClO, we anticipated that the strongly oxidized HClO can first oxidize the double bond between the SA-C2 moiety and pyrene moiety, then gradually hydrolyze into **SA-C2-CHO** and pyrene-CHO (Scheme S3, ESI†). The newly produced pyrene-CHO would form excimers in aqueous solution.[27] Therefore, the change in the F_{475}/F_{620} ratio can be linked to the response of **SA-C2-PCD** toward HClO, as shown in Fig. 2A. This proposed response mechanism was further confirmed by MS measurements. As expected, the mass peak at 730.4 m/z which corresponds to the nanoprobe **SA-C2-PCD** was replaced by mass peaks at 531.3 m/z and 231.1 m/z that correspond to **SA-C2-CHO** and pyrene-CHO, respectively (Fig. S12A and B, ESI†). These results supported the proposed reaction mechanism (Scheme S3, ESI†).

Imaging exogenous and endogenous HClO levels in living cells

We firstly evaluated the cytotoxicity of **AIED-Lyso** with representative HeLa cells (Fig. S13, ESI†). Positive results indicated minimal cytotoxicity and our **AIED-Lyso** should be suitable for intracellular HClO sensing.

This journal is © The Royal Society of Chemistry and the Chinese Chemical Society 2019

Mater. Chem. Front., 2019, **3**, 203–208 | 205
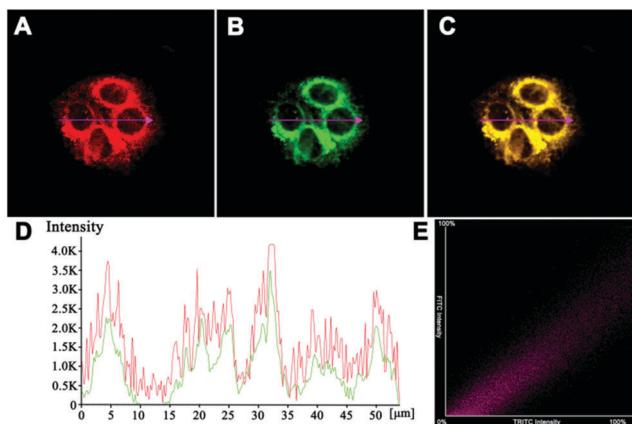
Fig. 4 Images of HeLa cells co-incubated with (A) **AIED-Lyso** (2.67 μg mL^{-1}; λ_{ex} = 405 nm, and λ_{em} = 575–675 nm) and (B) LysoTracker Green (500 nM; λ_{ex} = 468 nm, and λ_{em} = 500–520 nm); (C) the merged image of (A and B); (D) the intensity profile of ROI across HeLa cells from the red and green channels; and (E) the correlation plot of two channels. Scale bar: 20 μm.

It has been well documented that small molecule-based probes with a morpholine moiety mainly accumulate in lysosomes;[21,49] meanwhile, the intracellular uptake of nanoparticles is generally performed by the endocytosis strategy and they are often located in lysosomes.[50–53] To increase the lysosomal targeting ability, we introduce morpholine groups onto the surface of the nanoparticles to sense HClO in lysosomes. To conduct the colocalization studies, HeLa cells were treated with both **AIED-Lyso** and LysoTracker Green (a commercial lysosomal tracker), and the results are given in Fig. 4.
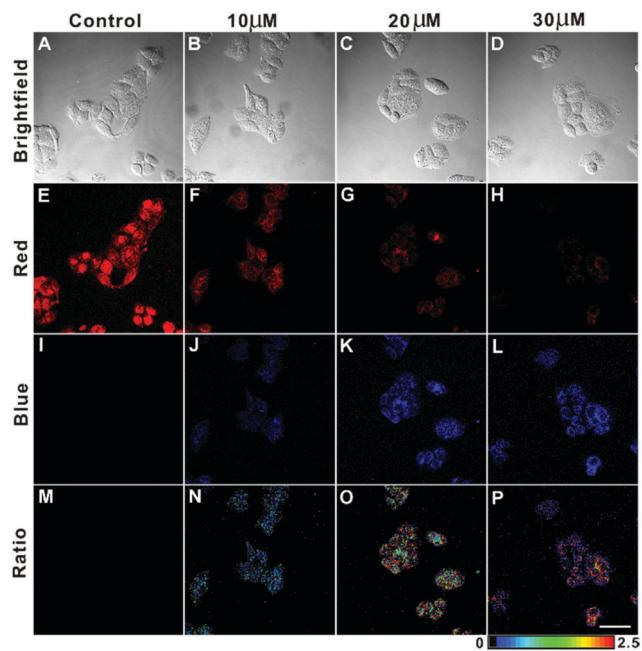
The red emission of **AIED-Lyso** fully overlapped with the green fluorescence of LysoTracker Green and the Pearson's R value was calculated to be 0.96 between our nanoprobe (shown in Red channel) and LysoTracker Green (shown in Green channel), which is far beyond the threshold of >0.5 required for correlation, indicating that **AIED-Lyso** mainly localized in lysosomes and can specifically monitor HClO in lysosomes.

AIED-Lyso was subsequently used for ratiometric imaging of exogenous HClO levels in HeLa cells. As shown in Fig. 5, HeLa cells treated with only **AIED-Lyso** provide strong red fluorescence and a low ratio of emission intensity (blue/red) (Fig. 5E, I and M). When the cells pre-treated with **AIED-Lyso** were exposed to different concentrations of HClO (10 μM, 20 μM and 30 μM), the blue fluorescence was obviously enhanced (Fig. 5J, K and L), accompanied by a decrease in red fluorescence (Fig. 5F, G and H). Accordingly, the ratio of emission intensity (blue/red) is also significantly enhanced (Fig. 5N, O and P). These results suggest that **AIED-Lyso** can be applied for ratiometric imaging of exogenous HClO in living cells.
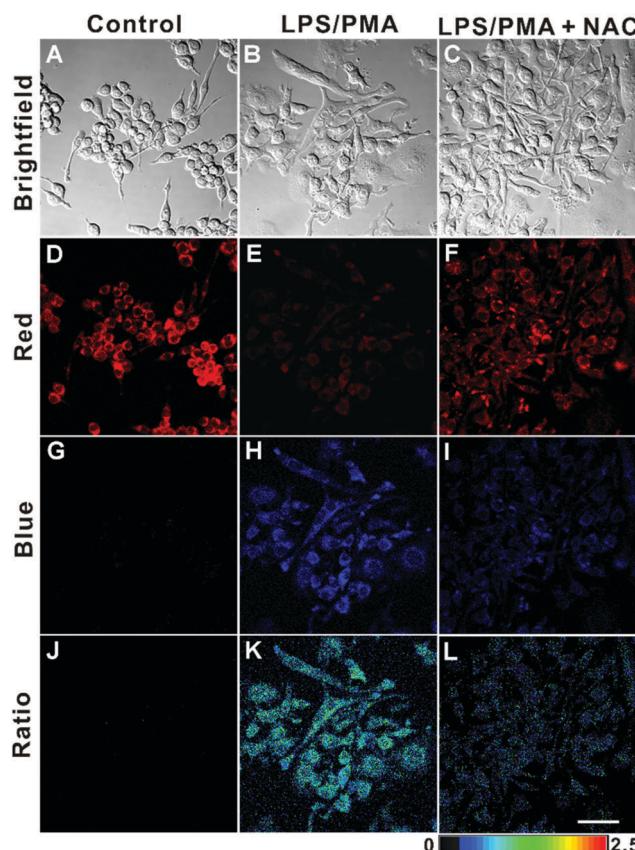
Fig. 6 Fluorescence microscopy images of RAW264.7 cells. The control groups (A, D and G) are incubated with **AIED-Lyso** (2.67 μg mL^{-1}) for 3 h. The cells in groups (B, E, and H) are first incubated with LPS (1 μg mL^{-1}) for 12 h, followed by coincubation with PMA (1 μg mL^{-1}) and **AIED-Lyso** (2.67 μg mL^{-1}) for 3 h. The cells in groups (C, F, and I) are first incubated with LPS (1 μg mL^{-1}) and NAC (2 mM) for 12 h, followed by coincubation with PMA (1 μg mL^{-1}) and **AIED-Lyso** (2.67 μg mL^{-1}) for 3 h. The ratio image is obtained as the ratio of blue fluorescence intensity to red fluorescence intensity (F_{blue}/F_{red}) (J, K and L). λ_{ex} = 405 nm, λ_{em1} = 425–525 nm (blue channel), and λ_{em2} = 575–675 nm (red channel), scale bar = 20 μm.

Fig. 5 Fluorescence images of HeLa cells treated with **AIED-Lyso** (2.67 μg mL^{-1}) with the addition of 0 (control), 10 μM, 20 μM and 30 μM HClO (from the left column to the right column). The ratio images were all obtained as F_{blue}/F_{red}. λ_{ex} = 405 nm, λ_{em1} = 425–525 nm (blue channel), and λ_{em2} = 575–675 nm (red channel), scale bar = 20 μm.

It was noted that the living cells were complicated systems, and the intracellular uptake of HClO was lower than the initial concentration. In addition, the intracellular reducing substances (e.g. GSH) can consume some of the HClO. Thus, a relatively high HClO concentration (10–30 μM) was applied to the cells in order to make the nanoprobe facile for ratiometric imaging of exogenous HClO levels in HeLa cells.

Finally, we imaged endogenous HClO in living cells. It has been well documented that endogenous HClO can be produced from RAW264.7 cells by treating them with lipopolysaccharide (LPS) and phorbol myristate acetate (PMA).[54,55] As illustrated in Fig. 6, the RAW264.7 cells incubated with only **AIED-Lyso** showed bright red fluorescence with a low ratio of emission intensity (blue/red) (Fig. 6D, G and J). After stimulating with LPS and PMA, the RAW264.7 cells treated with **AIED-Lyso** revealed an obvious decrease in red fluorescence but a significant enhancement in blue fluorescence with a high ratio of emission intensity (blue/red) (Fig. 6E, H and K). To further confirm that the intracellular fluorescence emission changes were triggered by the endogenous HClO, N-acetylcysteine (NAC) was added as an effective ROS scavenger to reduce the cellular HClO level.[56,57] As shown in Fig. 6F, I and L, when the RAW264.7 cells were incubated with LPS, PMA and NAC, the blue fluorescence was suppressed, whereas the red fluorescence was recovered to some extent. The above results demonstrated that **AIED-Lyso** can serve as a ratiometric nanoprobe to visualize the endogenously generated HClO in RAW264.7 cells.

Conclusions

In summary, a novel lysosome-targetable and ratiometric nanoprobe (**AIED-Lyso**) was rationally designed and synthesized for selectively sensing exogenous and endogenous HClO levels in live cells. The results indicated that **AIED-Lyso** possessed stable water dispersity, high selectivity, excellent long-term fluorescence stability (>10 weeks), and good biocompatibility. Importantly, with the aid of the lysosomal targeting group, **AIED-Lyso** can mainly accumulate in lysosomes and then monitor the exogenous and endogenous HClO in live cells. The design of the lysosome-targetable and ratiometric fluorescent nanoprobe presented herein should provide a new avenue for exploring the function of HClO-associated diseases.

Conflicts of interest

The authors declare no competing financial interest.

Acknowledgements

Notes and references

1 Z. M. Prokopowicz, F. Arce, R. Biedron, C. L.-L. Chiang, M. Ciszek, D. R. Katz, M. Nowakowska, S. Zapotoczny, J. Marcinkiewicz and B. M. Chain, *J. Immunol.*, 2010, **184**, 824–835.

2 Y. W. Yap, M. Whiteman and N. S. Cheung, *Cell. Signalling*, 2007, **19**, 219–228.

3 M. Singh, M. Arseneault, T. Sanderson, V. Murthy and C. Ramassamy, *J. Agric. Food Chem.*, 2008, **56**, 4855–4873.

4 M. J. Steinbeck, L. J. Nesti, P. F. Sharkey and J. Parvizi, *J. Orthop. Res.*, 2007, **25**, 1128–1135.

5 G. Kroemer and M. Jäättelä, *Nat. Rev. Cancer*, 2005, **5**, 886.

6 F. Yu, Z. Chen, B. Wang, Z. Jin, Y. Hou, S. Ma and X. Liu, *Tumor Biol.*, 2016, **37**, 1427–1436.

7 P. R. Pryor and J. P. Luzio, *Biochim. Biophys. Acta, Mol. Cell Res.*, 2009, **1793**, 615–624.

8 S. J. Klebanoff, *J. Leukocyte Biol.*, 2005, **77**, 598–625.

9 L. Yuan, L. Wang, B. K. Agrawalla, S. Park, H. Zhu, B. Sivaraman, J. Peng, Q. Xu and Y. Chang, *J. Am. Chem. Soc.*, 2015, **137**, 5930–5938.

10 X. Li, X. Gao, W. Shi and H. Ma, *Chem. Rev.*, 2014, **114**, 590–659.

11 Y. Yang, Q. Zhao, W. Feng and F. Li, *Chem. Rev.*, 2013, **113**, 192–270.

12 P. Zhang, Y. Tian, H. Liu, J. Ren, H. Wang, R. Zeng, Y. Long and J. Chen, *Chem. Commun.*, 2018, **54**, 7231–7234.

13 M. Gao, F. Yu, C. Lv, J. Choo and L. Chen, *Chem. Soc. Rev.*, 2017, **46**, 2237–2271.

14 L. He, B. Dong, Y. Liu and W. Lin, *Chem. Soc. Rev.*, 2016, **45**, 6449–6461.

15 V. S. Lin, W. Chen, M. Xian and C. J. Chang, *Chem. Soc. Rev.*, 2015, **44**, 4596–4618.

16 F. Gouanvé, T. Schuster, E. Allard, R. Méallet-Renault and C. Larpent, *Adv. Funct. Mater.*, 2007, **17**, 2746–2756.

17 P. Zhang, X. F. Jiang, X. Nie, Y. Huang, F. Zeng, X. Xia and S. Wu, *Biomaterials*, 2016, **80**, 46–56.

18 X. P. He, X. L. Hu, T. D. James, J. Yoon and H. Tian, *Chem. Soc. Rev.*, 2017, **46**, 6687–6696.

19 X. Jiao, Y. Li, J. Niu, X. Xie, X. Wang and B. Tang, *Anal. Chem.*, 2018, **90**, 533–555.

20 X. Chen, F. Wang, J. Y. Hyun, T. Wei, J. Qiang, X. Ren, I. Shin and J. Yoon, *Chem. Soc. Rev.*, 2016, **45**, 2976–3016.

21 M. Ren, K. Zhou, L. He and W. Lin, *J. Mater. Chem. B*, 2018, **6**, 1716–1733.

22 M. H. Lee, J. S. Kim and J. L. Sessler, *Chem. Soc. Rev.*, 2015, **44**, 4185–4191.

23 H. Zhu, J. Fan, J. Wang, H. Mu and X. Peng, *J. Am. Chem. Soc.*, 2014, **136**, 12820–12823.

24 W. Chen, A. Pacheco, Y. Takano, J. J. Day, K. Hanaoka and M. Xian, *Angew. Chem., Int. Ed.*, 2016, **55**, 9993–9996.

This journal is © The Royal Society of Chemistry and the Chinese Chemical Society 2019

Mater. Chem. Front., 2019, **3**, 203–208 | 207

25 W. Chen, E. W. Rosser, T. Matsunaga, A. Pacheco, T. Akaike and M. Xian, *Angew. Chem., Int. Ed.*, 2015, **54**, 13961–13965.

26 X. Zhang, W. Zhao, B. Li, W. Li, C. Zhang, X. Hou, J. Jiang and Y. Dong, *Chem. Sci.*, 2018, **9**, 8207–8212.

27 Y. Wu, J. Wang, F. Zeng, S. Huang, J. Huang, H. Xie, C. Yu and S. Wu, *ACS Appl. Mater. Interfaces*, 2016, **8**, 1511–1519.

28 M. Xue, H. Wang, J. Chen, J. Ren, S. Chen, H. Yang, R. Zeng, Y. Long and P. Zhang, *Sens. Actuators, B*, 2018, **282**, 1–9.

29 Y. Huang, P. Zhang, M. Gao, F. Zeng, A. Qin, S. Wu and B. Z. Tang, *Chem. Commun.*, 2016, **52**, 7288–7291.

30 J. Chen, C. Zhang, K. Lv, H. Wang, P. Zhang, P. Yi and J. Jiang, *Sens. Actuators, B*, 2017, **251**, 533–541.

31 S. Shen, X. Zhao, X. Zhang, X. Liu, H. Wang, Y. Dai, J. Miao and B. Zhao, *J. Mater. Chem. B*, 2017, **5**, 289–295.

32 H. Wang, P. Zhang, Y. Hong, B. Zhao, P. Yi and J. Chen, *Polym. Chem.*, 2017, **8**, 5795–5802.

33 P. Zhang, H. Wang, D. Zhang, X. Zeng, R. Zeng, L. Xiao, H. Tao, Y. Long, P. Yi and J. Chen, *Sens. Actuators, B*, 2018, **255**, 2223–2231.

34 P. Zhang, H. Wang, Y. Hong, M. Yu, R. Zeng, Y. Long and J. Chen, *Biosens. Bioelectron.*, 2018, **99**, 318–324.

35 P. Zhang, X. Nie, M. Gao, F. Zeng, A. Qin, S. Wu and B. Z. Tang, *Mater. Chem. Front.*, 2017, **1**, 838–845.

36 J. Liang, B. Z. Tang and B. Liu, *Chem. Soc. Rev.*, 2015, **44**, 2798–2811.

37 J. Qian and B. Z. Tang, *Chemistry*, 2017, **3**, 56–91.

38 D. Ding, K. Li, B. Liu and B. Z. Tang, *Acc. Chem. Res.*, 2013, **46**, 2441–2453.

39 H. Li, J. Chang, T. Hou and F. Li, *J. Mater. Chem. B*, 2016, **4**, 198–201.

40 W. Zhong, X. Zeng, J. Chen, Y. Hong, L. Xiao and P. Zhang, *Polym. Chem.*, 2017, **8**, 4849–4855.

41 Z. Guo, A. Shao and W.-H. Zhu, *J. Mater. Chem. C*, 2016, **4**, 640–2646.

42 A. Shao, Y. Xie, S. Zhu, Z. Guo, S. Zhu, J. Guo, P. Shi, T. D. James, H. Tian and W. H. Zhu, *Angew. Chem., Int. Ed.*, 2015, **54**, 7275–7280.

43 X. Zhang, K. Wang, M. Liu, X. Zhang, L. Tao, Y. Chen and Y. Wei, *Nanoscale*, 2015, **7**, 11486–11508.

44 D. Wang, J. Qian, W. Qin, A. Qin, B. Z. Tang and S. He, *Sci. Rep.*, 2014, **4**, 4279.

45 G. Feng, W. Wu, S. Xu and B. Liu, *ACS Appl. Mater. Interfaces*, 2016, **8**, 21193–21200.

46 Q. Ye, S. Chen, D. Zhu, X. Lu and Q. Lu, *J. Mater. Chem. B*, 2015, **3**, 3091–3097.

47 K. Li, Z. Zhu, P. Cai, R. Liu, N. Tomczak, D. Ding, J. Liu, W. Qin, Z. Zhao, Y. Hu, X. Chen, B. Z. Tang and B. Liu, *Chem. Mater.*, 2013, **25**, 4181–4187.

48 P. Zhang, Y. Hong, H. Wang, M. Yu, Y. Gao, R. Zeng, Y. Long and J. Chen, *Polym. Chem.*, 2017, **8**, 7271–7278.

49 W. Xu, Z. Zeng, J.-H. Jiang, Y.-T. Chang and L. Yuan, *Angew. Chem., Int. Ed.*, 2016, **55**, 13658–13699.

50 C. Zhu, D. Huo, Q. Chen, J. Xue, S. Shen and Y. Xia, *Adv. Mater.*, 2017, 1703702.

51 F. Du, Y. Ming, F. Zeng, C. Yu and S. Wu, *Nanotechnology*, 2013, **24**, 365101.

52 X. Ma, X. Wu, S. Jin, Y. Tian, X. Zhang, Y. Zhao, L. Yu and X.-J. Liang, *ACS Nano*, 2011, **5**, 8629–8639.

53 Y. Hong, P. Zhang, H. Wang, M. Yu, Y. Gao and J. Chen, *Sens. Actuators, B*, 2018, **272**, 340–347.

54 Y. Koide, Y. Urano, K. Hanaoka, T. Terai and T. Nagano, *J. Am. Chem. Soc.*, 2011, **133**, 5680–5682.

55 W. Zhang, W. Liu, P. Li, J. Kang, J. Wang, H. Wang and B. Tang, *Chem. Commun.*, 2015, **51**, 10150–10153.

56 Z. Zhan, R. Liu, L. Chai, Q. Li, K. Zhang and Y. Lv, *Anal. Chem.*, 2017, **89**, 9544–9551.

57 Y. W. Jun, S. Sarkar, S. Singha, Y. J. Reo, H. R. Kim, J. Kim, Y. Chang and K. H. Ahn, *Chem. Commun.*, 2017, **53**, 10800–10803.